A novel cuproptosis-related gene signature can predict prognosis in acute myeloid leukemia

Xuan Zhou
Nanjing Drum Tower Hospital
Zhenzhen Xu
Nanjing Drum Tower Hospital
Hehua Ma
Nanjing Drum Tower Hospital
Zuyi Weng
Nanjing Drum Tower Hospital
Juan Li (juanli2003@163.com)
Nanjing Drum Tower Hospital

Research Article

Keywords: Acute myeloid leukemia, cuproptosis, prognostic gene signature, overall survival, immune cell infiltration

Posted Date: May 10th, 2022

DOI: https://doi.org/10.21203/rs.3.rs-1628980/v1

Abstract

Acute myeloid leukemia (AML) is the most common and lethal acute leukemia in adults with a dismal prognosis. Infiltrating immune significantly affects the progression of AML. Cuproptosis is a copper-dependent programmed cell death. However, the prognostic significance of cuproptosis-related genes (CRGs) remains unclear. In this study, we evaluated prognostic value of each CRGs and constructed a 3-gene risk model using RNA-sequencing data of AML from The Cancer Genome Atlas (TCGA) cohort. Each AML sample was calculated with a risk score based on the risk model, and then assigned into low- and high-risk groups. Patients with a high risk-score exhibited much worse overall survival. These findings were verified in a Gene Expression Omnibus (GEO) database. Functional analysis indicated that immune status differed between low- and high-risk groups, as well as immune cell infiltration and drug sensitivity. In summary, the risk model based on the expression of CRGs is a promising prognostic biomarker for AML.

Introduction

AML is a kind of malignant blood diseases originating from uncontrolled proliferation of hematopoietic progenitors in bone marrow. AML is the most common type of adult leukemia. The therapeutic approaches of AML have not made much development over the past decades. The outcome of AML remains unsatisfactory with overall survival (OS) under 40% [1]. Thus, it is urgent to explore molecular basis of AML and identify novel prognostic biomarkers, which may contribute to a better treatment strategy as well as better outcomes of AML patients.

Transition metals like Fe, Mn, Cu, and Zn are essential trace elements across all forms of life [2–4]. These metal ions are utilized as critical enzymatic cofactors, and participate in cell functions such as electron transfer and signaling pathways. However, these transition metals can be toxic in excess. Appropriate levels of metal ions in organisms are tightly maintained through multiple regulatory pathways.

Cuproptosis is a newly-proposed concept published in the journal Science this year [5]. It is a copper-dependent programmed cell death characterized by protein lipoylation in the tricarboxylic acid (TCA) cycle. It is a distinct form of cell death pathways, which differs from apoptosis, necrosis, autophagy, and ferroptosis. FDX1 is the key regulator in the process of cuproptosis and regulates protein lipoylation [6]. Copper is transported into mitochondria and binds the lipoylated TCA enzymes directly [7, 8]. As a result, acute proteotoxic stress was induced by lipoylated protein aggregation and subsequently loss of Fe-S cluster-containing proteins. This study demonstrates that cells depend on mitochondrial respiration would be more sensitive to cuproptosis. These findings may be a new way of treating cancer cells. Actually, depletion of mitochondrial copper has been proved effective against triple-negative breast cancer which depends on oxidative phosphorylation [9].

Given the current findings, we suppose that cuproptosis may have an important role in the development of AML. However, its specific functions have never been studied. In this study, we performed a systematic

analysis to determine the expression levels of cuproptosis-related genes in AML, explore the prognostic value of these genes, and discuss the correlations between cuproptosis and the tumor immune microenvironment.

Materials And Methods

1. Data collection from TCGA and GEO datasets

The RNA sequencing (RNA-seq) data of AML patients from TCGA database were obtained via the Cbioportal website (https://www.cbioportal.org/study/summary?id=laml_tcga_pub), along with their corresponding clinical features. We excluded AML samples with no record of overall survival or living status, or if their survival time was no longer than 0 days. Meanwhile, 70 samples of K562 cells – leukemia cell line – from GTEx database (https://xenabrowser.net/datapages/) were used as normal controls and their RNA-seq data were downloaded. In addition, the Series Matrix File of GSE37642, containing complete survival data, was retrieved from GEO (https://www.ncbi.nlm.gov/geo/).

2. Establishment and verification of a cuproptosis-related gene prognostic signature

We conducted least absolute shrinkage and selection operator (LASSO)-penalized Cox regression analyses to explore the prognostic value of cuproptosis-related genes [10]. An R package “glmnet” was utilized to establish a prognostic model. LASSO regression was performed using a 10-fold cross-validation and the penalty parameter (λ) was set to the minimum criteria. The risk scores were calculated based on the results of LASSO regression. AML patients from TCGA were defined according to the median risk score as low- and high-risk subgroups. Kaplan-Meier survival analysis was performed to compare differences in OS between the two subgroups. Moreover, time-dependent receiver operating characteristic (ROC) curves were constructed with “timeROC” R package. The GSE37642 dataset was then employed for validation of the gene prognostic signature.

Univariable and multivariable Cox regression analyses were performed in order to determine associations of risk score with clinical features such as age, gender, and FAB subtype. The result was also validated in the GEO cohort.

3. Functional analysis of differentially expressed genes (DEGs) between low- and high-risk subgroups

The R package “limma” was applied to identify DEGs between the two subgroups of AML patients from TCGA cohort. The criteria were set as $|logFC| > 1$ and $adj.P.value < 0.05$. Then Gene ontology (GO) and

Kyoto Encyclopedia of Genes and Genomes (KEGG) enrichment analyses were carried out through “clusterProfiler” package [11].

A protein-protein interaction (PPI) network was constructed based on Search Tool for the Retrieval of Interacting Genes (STRING) network [12], and further visualized in Cytoscape software (version 3.8.2). The top 3 nodes were selected as hub genes based on scores calculated by the maximal clique centrality (MCC) method of cytoHubba, a plug-in in Cytoscape.

4. Prediction of clinical chemotherapeutic response

To predict differences of clinical chemotherapeutic response between low- and high-risk AML subgroups in the TCGA cohort, we applied the pRRophetic algorithm [13] on R based on the Genomics of Drug Sensitivity in Cancer (GDSC) database (https://www.cancer-rxgene.org/) [14]. The IC50 values were evaluated and compared between the two subgroups using Wilcoxon signed-rank test.

5. Evaluation of immune cell infiltration

To determine the proportion of tumor-infiltrating immune cells (TIICs) in the AML subgroups, CIBERSORT algorithm was performed [15]. The immune cell infiltration was measured by single-sample gene set enrichment analysis (ssGSEA). Correlation analysis was evaluated by Spearman. P value < 0.05 was considered significant.

6. Statistical analysis

Analyses were performed using R (version 4.1.2) as mentioned above. SPSS software was utilized to analyze clinical features of AML patients. A p value less than 0.05 was generally considered statistically significant unless otherwise specified.

Results

1. Expression of cuproptosis-related genes (CRGs) in AML patients

A total of 172 AML patients in TCGA database were enrolled in this analysis after filtered as mentioned above. In addition, 136 samples from GSE37642 cohort were recruited as validation group. The detailed clinical information (age, gender, FAB subtype, WBC, etc.) for TCGA and GSE37642 cohorts were gathered and listed in Table 1.

Table 1

Clinical characteristics of AML patients in TCGA and GEO cohorts.

Characteristics	TCGA	GSE37642
Gender (number)		
Male	92	
Female	80	
Age (years)		
Median	58	59.5
Range	18-88	18-85
FAB (number)		
M0	16	8
M1	44	29
M2	38	47
M3	16	7
M4	34	17
M5	17	19
M6	2	7
M7	3	1
NA	2	1
WBC		
Median	16.5	
Range	0.4-297.4	
BM-BLAST		
Median	72.5	
Range	30-100	
Living status (number)		
Dead	113	98
Alive	59	38
Overall survival (months)		
Median	17.25	14.68
Range	0.1-118.1	0.07-130.63

We extracted 14 CRGs through screening relative articles published. The expression of CRGs in AML patients were compared with 70 control samples from GTEx database. As seen in Fig. 1a, ATP7A, ATP7B, DLAT, DLD, FDX1, GCSH, LIAS, PDHA1, SLC25A3, and SLC31A1 were decreased, while DBT, DLST and LIPT1 were increased with P values all less than 0.001. No obvious difference was found in PDHB expression.

2. Prognostic values of CRGs in TCGA AML cohort

Next, we explored the prognostic values of CRGs. Kaplan-Meier analyses were performed for each CRGs in TCGA AML cohort and the results were visualized as forest plots to display P values and hazard ratios (HR). According to the forest plots, patients with a low-expression of GCSH or LIPT1, or a high-expression of DLAT exhibited markedly worse overall survival rate (Fig. 1b).

3. Construction of a prognostic gene signature in AML

Since PDHB showed no difference of expression in AML patients compared with controls, only 13 CRGs were retained for further analysis except for PDHB. LASSO Cox regression analysis was applied to develop a prognostic model. As a result, a 3-gene signature was generated (Fig. 2a, b). The risk score was calculated through the following formula: risk score = (-0.01161) * GCSH expression + (-0.40387) * LIPT1 expression + (0.248985) * PDHA1 expression.

To evaluate the performance of the 3-gene signature, 172 AML patients from TCGA were stratified equally into low- and high-risk subgroups based on the median score calculated by the formula (Fig. 2c). Patients in the latter group had more deaths than in the former group (Fig. 2d). In addition, Kaplan-Meier analysis revealed that the OS time was notably different between the two groups. Relative to high-risk group, patients in low-risk group had an advantage of higher OS (P = 0.003, Fig. 2e). We further performed time dependent ROC analysis to evaluate the specificity and sensitivity of the gene signature. The area under the ROC curve (AUC) was 0.665, 0.644 and 0.611 for 1, 2, and 3-year survival, separately (Fig. 2f).

We next evaluated whether the risk model could serve as an independent prognostic factor. As shown in Fig. 2g and h, both the univariate and multivariate Cox regression analyses implied that the risk score was an independent prognostic factor (p = 0.0034, 0.0027, separately). These results demonstrated that a high risk-score was able to predict independently poor survival of AML patients.

4. Validation of the risk model in GEO datasets

GSE37642 cohort was utilized as external validation. A total of 136 AML patients were classified equally into the low- and high-risk groups according to the median risk score calculated (Fig. 3a). Same to the TCGA cohort, patients who had a high risk-score in GSE37642 were observed to have shorter survival times than those in low-risk group (Fig. 3b). The OS rate in high-risk group was significantly poorer than

in low-risk group, as the Kaplan-Meier curves indicated (P = 0.0216, Fig. 3c). In addition, time dependent ROC analysis showed similar AUC: 0.602, 0.621 and 0.636 for 1, 2, and 3-year survival, separately (Fig. 3d).

5. Functional analysis of DEGs between low- and high-risk groups

To further explore risk score-associated differences of gene expression and biological functions and pathways, we screened for DEGs between the two subgroups using R package “limma”. The criteria were set as mentioned above, and as a result, 240 genes were identified. Among them, 159 genes were upregulated while 81 were downregulated in the high-risk group. The result was displayed in a volcano plot (Fig. 4a).

As shown in Fig. 4b & c, GO and KEGG functional enrichment analysis were performed. The 240 DEGs were mainly enriched in the following terms or pathways: positive regulation of inflammatory response, amide binding, peptide binding, osteoclast differentiation, and B cell receptor signaling pathway, etc.

A PPI network of 240 DEGs were constructed in STRING database and analyzed in Cytoscape software. The top 3 nodes of most importance were selected: S100A9, S100A8, and LILRB2 (Fig. 4d).

6. Prediction of drug sensitivity based on the risk model

We further tested the impact of risk score on cells’ response to different drugs based on GDSC drug sensitivity data. A total of 41 drugs were found to have a significant difference of IC50 values between low- and high-risk groups. AML patients in the high-risk group showed a worse response to all of the 41 drugs, the top 5 of which were Parthenolide, SL.0101.1, Sunitinib, KU.55933, and RDEA119, with P values of 7.71E-06, 1.49E-05, 4.99E-05, 1.07E-04, and 1.21E-04, separately (Fig. 5a).

7. Results of immune cell infiltration analysis

The immune cell infiltration analysis was also performed to evaluate the correlation of risk scores with immune cells and immune-related pathways in the TCGA cohort. We discovered that aDCs, pDCs, and tumour-infiltrating lymphocytes (TILs) were significantly enriched in the high-risk group (Fig. 5b). Compared to the low-risk group, some immune pathways were upregulated in high-risk group, such as APC co-inhibition, CCR, Check-point, HLA, MHC class Ⅰ, Parainflammation, and T cell co-inhibition (Fig. 5c).

Discussion

Cuproptosis is a novel form of programmed cell death. Less is known about its role in leukemia. In this study, we compared the mRNA levels of a total of 14 CRGs. Most of them showed a different expression between AML patients and normal controls. Three genes including GCSH, LIPT1, and DLAT were observed with significant prognostic value separately. To further explore the role of cuproptosis in AML, we constructed a formula via LASSO Cox regression analysis based on the expression of 3 genes: GCSH, LIPT1, and PDHA1. The 3-gene signature had a good performance in prediction of diagnosis and prognosis of AML in TCGA cohort. In particular, a high risk-score was related with a poor outcome. The results were further validated in another cohort from GEO database. GCSH encodes an enzyme which could be lipoylated by FDX1 for activation. GCSH was reduced in AML and soft tissue sarcoma [16] while it was reported elevated in breast cancer tissues [17]. LIPT1 participates in lipoic acid metabolism pathway [18]. Recent evidence demonstrates that LIPT1 works to transfer lipoic acid moieties from one to another protein. PDHA1 is a component of the pyruvate dehydrogenase complex regulating pyruvate into the TCA cycle [19]. LIPT1 and GCSH acted as tumor suppressor genes. High expression of these two genes were correlated with better prognosis. How these genes work in the process of cuproptosis needs further investigation.

We analyzed DEGs in AML subgroups based on risk score and found that cuproptosis may interact with inflammatory responses. GO and KEGG analysis indicated the DEGs were mainly enriched in inflammation of immune response. In addition, B cell receptor signaling pathway was also enriched. The top 3 genes identified through PPI network were all related to immune response. Among them, LILRB2 was the gene of our most interest. LILRB2 is a member of the leukocyte immunoglobulin-like receptor (LIR) family expressed on cells of the myeloid lineage. Dendritic cells including aDCs and pDCs belong to myeloid cells. They were enriched in high-risk group through immune cell infiltration analysis. In agreement with upregulation of Check-point and MHC class immune pathways in high-risk group, LILRB2/MHC- serves as an innate immune checkpoint [20, 21].

LILRB2 has been reported to be involved in various cancer types. It has been observed that LILRB2 promote tumor cell proliferation and migration in several cancer types [22]. Some studies have also shown a positive relationship between LILRB2 expression and prognosis [23, 24]. It has attracted much attention developing drugs targeting LILRB2. Treatment with LILRB2 inhibitors could avoid immune evasion. Its combination with PD-1/PD-L1 inhibitors could avoid emerging of drug resistance. Two LILRB2 inhibitors, JTX-8064 and IO-108, are currently entering clinical trials (NCT04669899, NCT05054348), and the results would be worth looking forward to.

Finally, drug sensitivity analysis was performed to explore potential therapeutic possibility of drugs. The results demonstrated AML patients with high risk-scores exerted a worse sensitivity against anti-tumor agents. Taken into consideration that cuproptosis showed a link with immune checkpoint, the inhibitors of which were not included in GDSC database, it was necessary to study the possible effects of LILRB2 inhibitors.

In summary, our research demonstrated that cuproptosis has a strong relationship with AML. The risk scores generated by 3-gene-signature could predict the prognosis of AML well. Further investigations should be done to explore the accuracy and significance of the gene model in AML.

Declarations

Acknowledgments

We thank the TCGA and GEO databases for the availability of the data.

Funding

This work was supported by the National Natural Science Foundation of China (31371399 and 81803132)

Competing Interests

The authors have no relevant financial or non-financial interests to disclose.

Author Contributions

All authors contributed to the study conception and design. Material preparation, data collection and analysis were performed by Zhou Xuan, Xu Zhenzhen and Ma Hehua. Ma Hehua prepared Table 1. Xu Zhenzhen prepared Fig. 3. The other figures were prepared by Zhou Xuan. The first draft of the manuscript was written by Zhou Xuan and Weng Zuyi and all authors commented on previous versions of the manuscript. All authors read and approved the final manuscript.

References

1. Carter J.L., Hege K., Yang J., Kalpage H.A., Su Y., Edwards H., Hüttemann M., Taub J.W., and Ge Y., *Targeting multiple signaling pathways: the new approach to acute myeloid leukemia therapy.* Signal Transduct Target Ther, 2020. **5**(1): p. 288.
2. Zygiel E.M. and Nolan E.M., *Transition Metal Sequestration by the Host-Defense Protein Calprotectin.* Annu Rev Biochem, 2018. **87**: p. 621-643.
3. Romano C.A., Zhou M., Song Y., Wysocki V.H., Dohnalkova A.C., Kovarik L., Paša-Tolić L., and Tebo B.M., *Biogenic manganese oxide nanoparticle formation by a multimeric multicopper oxidase Mnx.* Nat Commun, 2017. **8**(1): p. 746.
4. Bafaro E., Liu Y., Xu Y., and Dempski R.E., *The emerging role of zinc transporters in cellular homeostasis and cancer.* Signal Transduct Target Ther, 2017. **2**: p. 17029-.
5. Tsvetkov P., Coy S., Petrova B., Dreishpoon M., Verma A., Abdusamad M., Rossen J., Joesch-Cohen L., Humeidi R., Spangler R.D., Eaton J.K., Frenkel E., Kocak M., Corsello S.M., Lutsenko S., Kanarek N.,

Santagata S., and Golub T.R., *Copper induces cell death by targeting lipoylated TCA cycle proteins.* Science, 2022. **375**(6586): p. 1254-1261.

6. Weger M., Weger B.D., Görling B., Poschet G., Yildiz M., Hell R., Luy B., Akcay T., Güran T., Dickmeis T., Müller F., and Krone N., *Glucocorticoid deficiency causes transcriptional and post-transcriptional reprogramming of glutamine metabolism.* EBioMedicine, 2018. **36**: p. 376-389.
7. Beaino W., Guo Y., Chang A.J., and Anderson C.J., *Roles of Atox1 and p53 in the trafficking of copper-64 to tumor cell nuclei: implications for cancer therapy.* J Biol Inorg Chem, 2014. **19**(3): p. 427-38.
8. Hatori Y., Yan Y., Schmidt K., Furukawa E., Hasan N.M., Yang N., Liu C.N., Sockanathan S., and Lutsenko S., *Neuronal differentiation is associated with a redox-regulated increase of copper flow to the secretory pathway.* Nat Commun, 2016. **7**: p. 10640.
9. Cui L., Gouw A.M., LaGory E.L., Guo S., Attarwala N., Tang Y., Qi J., Chen Y.S., Gao Z., Casey K.M., Bazhin A.A., Chen M., Hu L., Xie J., Fang M., Zhang C., Zhu Q., Wang Z., Giaccia A.J., Gambhir S.S., Zhu W., Felsher D.W., Pegram M.D., Goun E.A., Le A., and Rao J., *Mitochondrial copper depletion suppresses triple-negative breast cancer in mice.* Nat Biotechnol, 2021. **39**(3): p. 357-367.
10. Tibshirani R., *The lasso method for variable selection in the Cox model.* Stat Med, 1997. **16**(4): p. 385-95.
11. Yu G., Wang L.G., Han Y., and He Q.Y., *clusterProfiler: an R package for comparing biological themes among gene clusters.* Omics, 2012. **16**(5): p. 284-7.
12. Szklarczyk D., Gable A.L., Nastou K.C., Lyon D., Kirsch R., Pyysalo S., Doncheva N.T., Legeay M., Fang T., Bork P., Jensen L.J., and von Mering C., *The STRING database in 2021: customizable protein-protein networks, and functional characterization of user-uploaded gene/measurement sets.* Nucleic Acids Res, 2021. **49**(D1): p. D605-d612.
13. Geeleher P., Cox N., and Huang R.S., *pRRophetic: an R package for prediction of clinical chemotherapeutic response from tumor gene expression levels.* PLoS One, 2014. **9**(9): p. e107468.
14. Yang W., Soares J., Greninger P., Edelman E.J., Lightfoot H., Forbes S., Bindal N., Beare D., Smith J.A., Thompson I.R., Ramaswamy S., Futreal P.A., Haber D.A., Stratton M.R., Benes C., McDermott U., and Garnett M.J., *Genomics of Drug Sensitivity in Cancer (GDSC): a resource for therapeutic biomarker discovery in cancer cells.* Nucleic Acids Res, 2013. **41**(Database issue): p. D955-61.
15. Chen B., Khodadoust M.S., Liu C.L., Newman A.M., and Alizadeh A.A., *Profiling Tumor Infiltrating Immune Cells with CIBERSORT.* Methods Mol Biol, 2018. **1711**: p. 243-259.
16. Gu H.Y., Zhang C., Guo J., Yang M., Zhong H.C., Jin W., Liu Y., Gao L.P., and Wei R.X., *Risk score based on expression of five novel genes predicts survival in soft tissue sarcoma.* Aging (Albany NY), 2020. **12**(4): p. 3807-3827.
17. Adamus A., Müller P., Nissen B., Kasten A., Timm S., Bauwe H., Seitz G., and Engel N., *GCSH antisense regulation determines breast cancer cells' viability.* Sci Rep, 2018. **8**(1): p. 15399.
18. Cronan J.E., *Progress in the Enzymology of the Mitochondrial Diseases of Lipoic Acid Requiring Enzymes.* Front Genet, 2020. **11**: p. 510.

19. Echeverri Ruiz N.P., Mohan V., Wu J., Scott S., Kreamer M., Benej M., Golias T., Papandreou I., and Denko N.C., *Dynamic regulation of mitochondrial pyruvate metabolism is necessary for orthotopic pancreatic tumor growth.* Cancer Metab, 2021. **9**(1): p. 39.
20. Lentz R.W., Colton M.D., Mitra S.S., and Messersmith W.A., *Innate Immune Checkpoint Inhibitors: The Next Breakthrough in Medical Oncology?* Mol Cancer Ther, 2021. **20**(6): p. 961-974.
21. Zhang Y. and Zheng J., *Functions of Immune Checkpoint Molecules Beyond Immune Evasion.* Adv Exp Med Biol, 2020. **1248**: p. 201-226.
22. Fan J., Li J., Han J., Zhang Y., Gu A., Song F., Duan J., Yin D., Wang L., and Yi Y., *Expression of leukocyte immunoglobulin-like receptor subfamily B expression on immune cells in hepatocellular carcinoma.* Mol Immunol, 2021. **136**: p. 82-97.
23. Fan J., Wang L., Chen M., Zhang J., Li J., Song F., Gu A., Yin D., and Yi Y., *Analysis of the expression and prognosis for leukocyte immunoglobulin-like receptor subfamily B in human liver cancer.* World J Surg Oncol, 2022. **20**(1): p. 92.
24. Chen Q.Y., Chen Y.X., Han Q.Y., Zhang J.G., Zhou W.J., Zhang X., Ye Y.H., Yan W.H., and Lin A., *Prognostic Significance of Immune Checkpoints HLA-G/ILT-2/4 and PD-L1 in Colorectal Cancer.* Front Immunol, 2021. **12**: p. 679090.

Figures

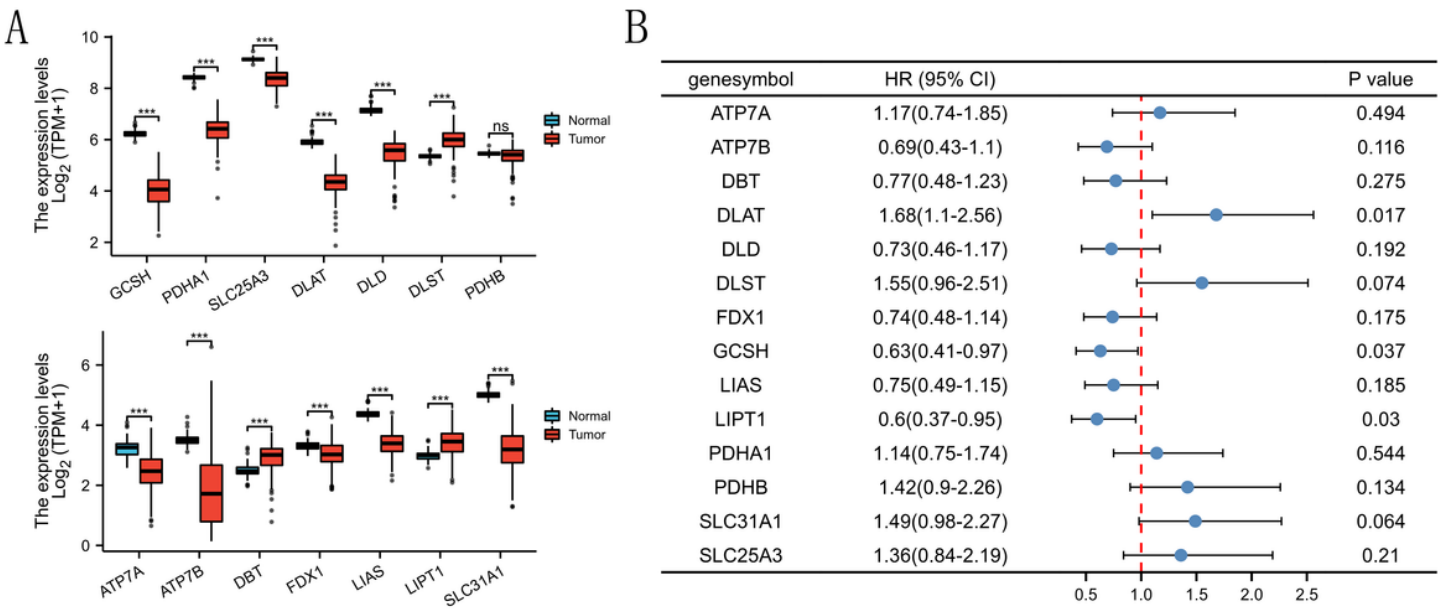

Figure 1

The expression and prognostic values of the CRGs in TCGA AML cohort. **a** The expression of 14 CRGs between AML patients and healthy control samples. **b** Forest plots of the prognostic values of 14 CRGs in AML cohort. *** p < 0.001.

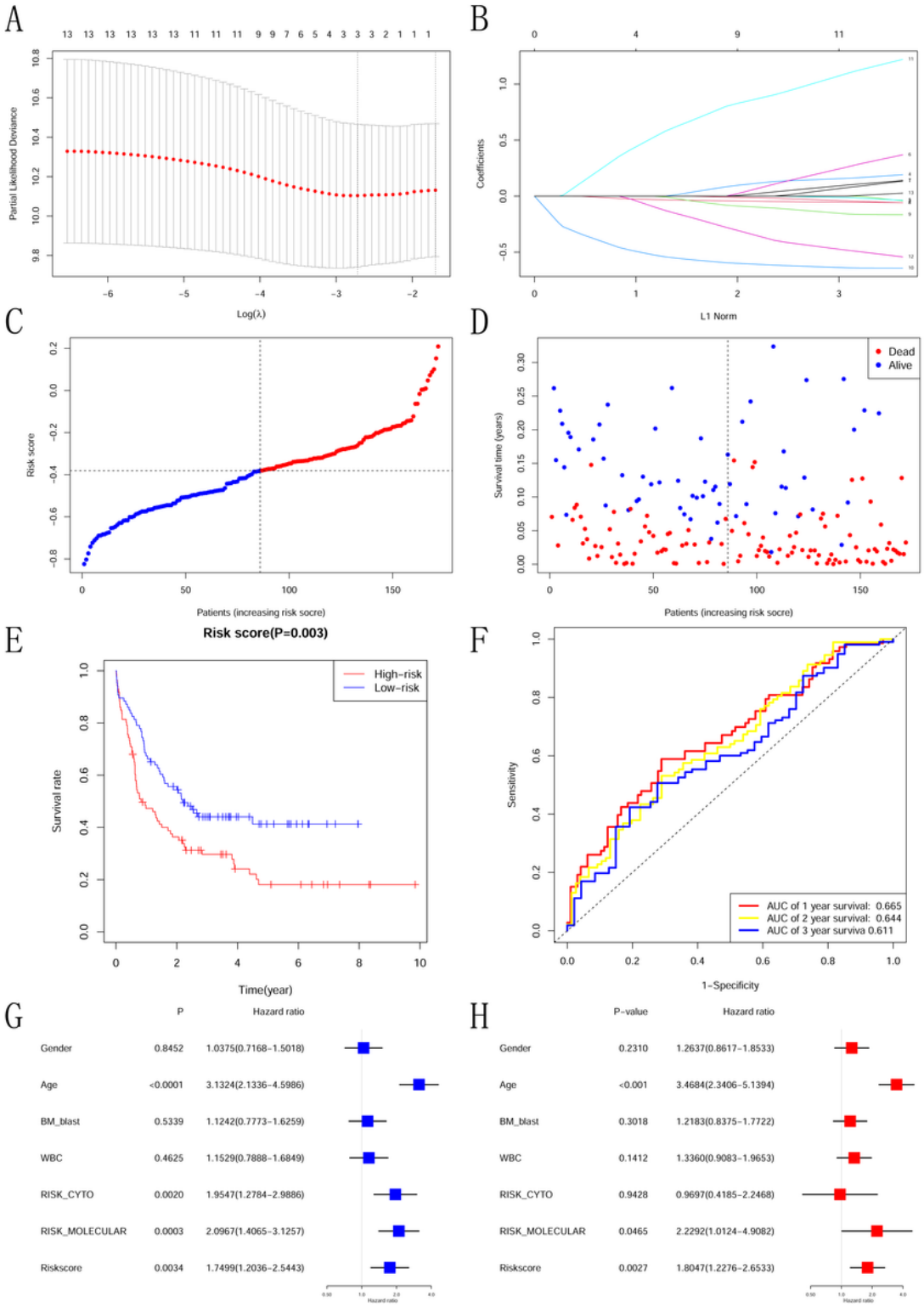

Figure 2

Construction of risk model in the TCGA cohort. **a** Ten-fold cross-validation for tuning parameter selection in the LASSO model. **b** LASSO regression analysis of the CRGs. **c** Distribution of patients based on the risk model. **d** The survival status for each patient (low-risk population: on the left side of the dotted line; high-risk population: on the right side of the dotted line). **e** Kaplan-Meier curves for the OS of patients in the low- and high-risk groups. **f** Time-dependent ROC curves demonstrated the predictive efficiency of the

risk score. **g** Univariate Cox regression analysis for the TCGA cohort. **h** Multivariate Cox regression analysis for the TCGA cohort.

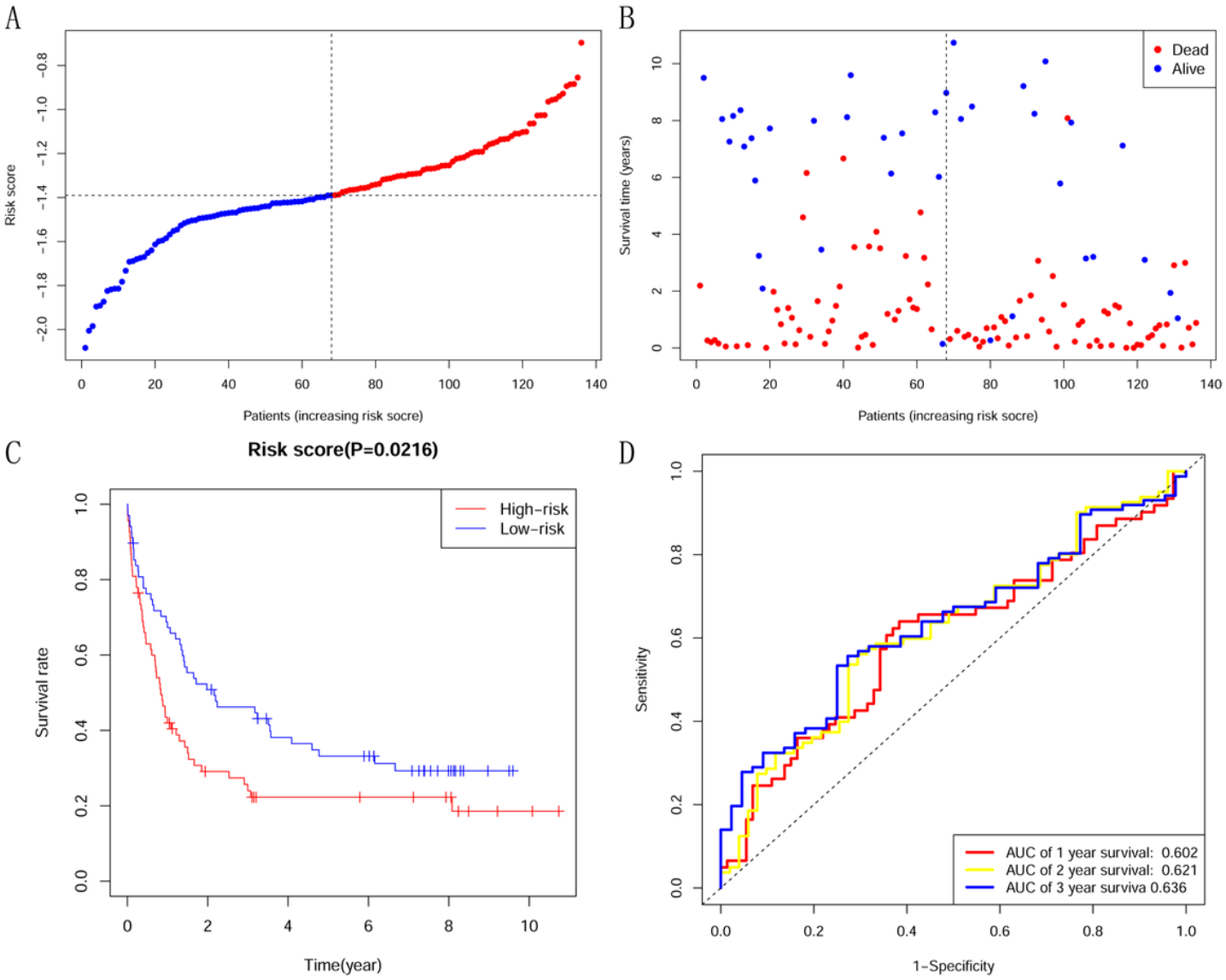

Figure 3

Validation of the risk signature in the GSE37642 cohort. **a** Distribution of patients in the GEO cohort based on the median risk score. **b** The survival status for each patient. **c** Kaplan–Meier curves for comparison of the OS between low- and high-risk groups. **d** Time-dependent ROC curves for OCs.

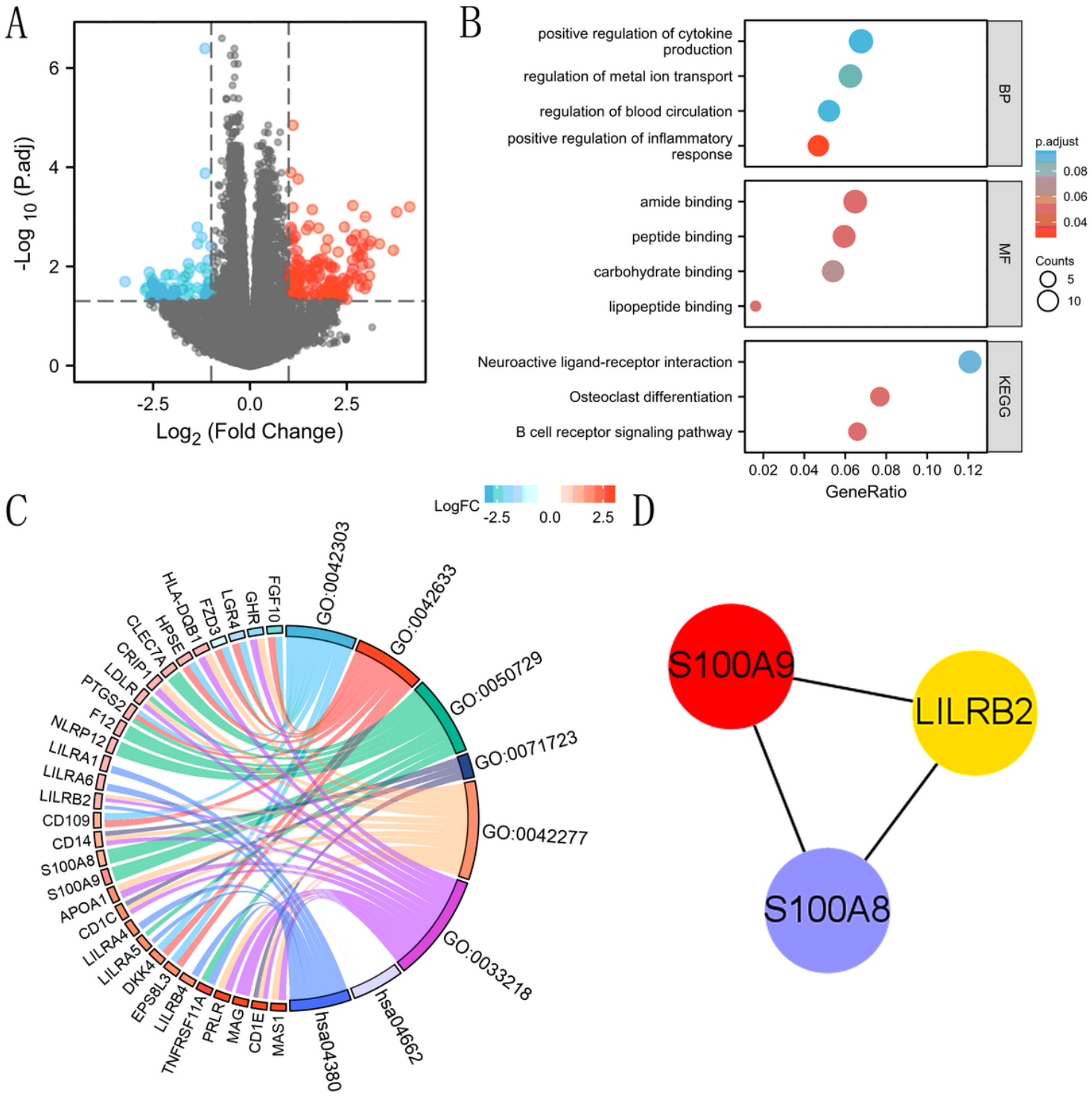

Figure 4

Functional analysis based on the DEGs between the two risk groups in the TCGA cohort. **a** Volcano plots of DEGs. **b** Bubble plots of GO-KEGG analysis. **c** Chord diagram of GO-KEGG analysis together with the expression status of each DEGs. **d** Top 3 hub genes identified through PPI analysis.

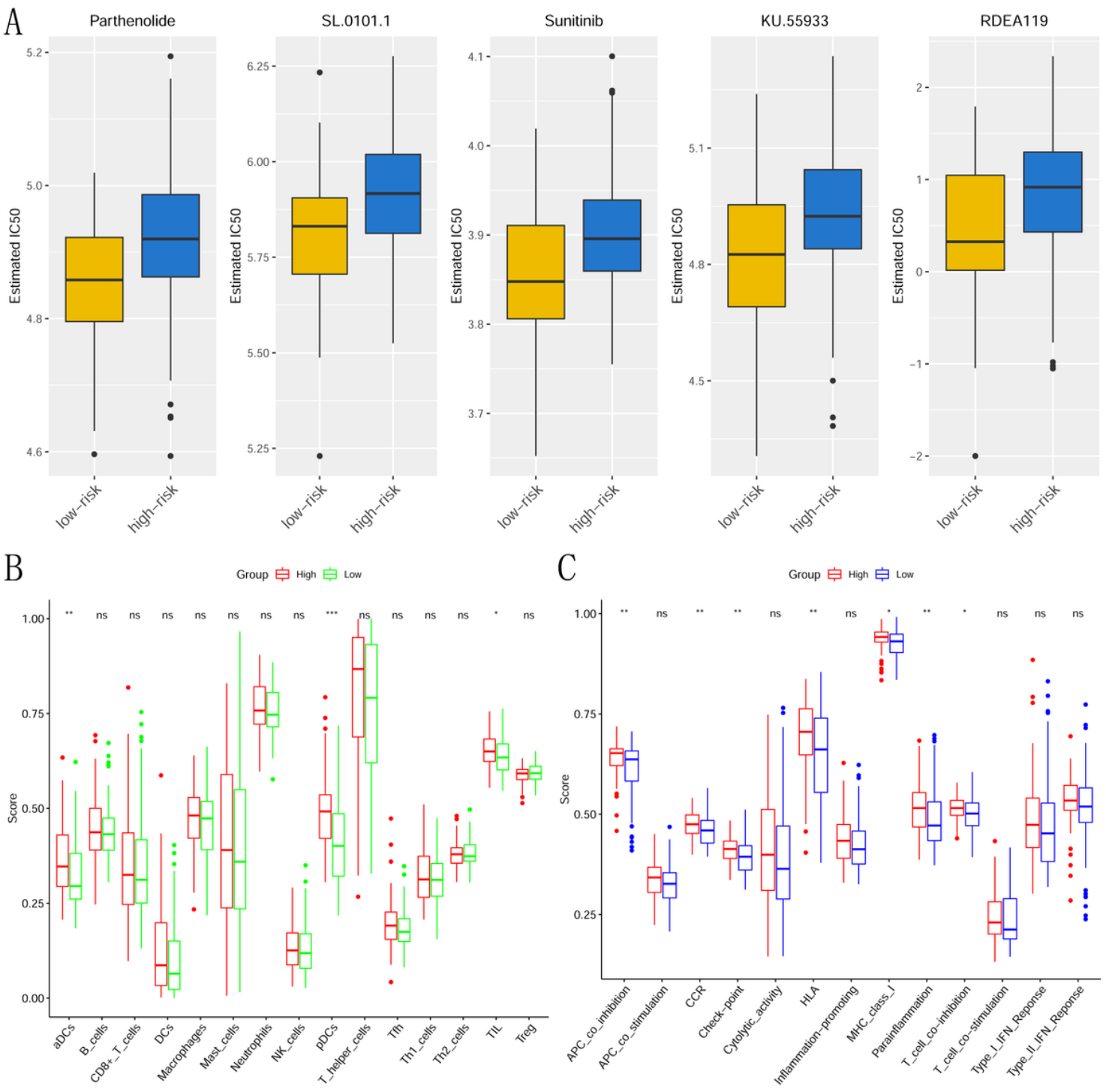

Figure 5

Prediction of drug sensitivity and immune cell infiltration analysis based on the risk model. **a** Box plot denote association between risk scores and the IC50 of various drugs on AML patients. **b & c** Comparison of the enrichment scores of 15 types of immune cells (**b**) and 13 immune-related pathways (**c**) between low- and high-risk group in the TCGA cohort.